

Numerical Tools for the Study of Instabilities within the Positive-Differential-Resistance Regions of Tunneling Devices

M. I. Lasater¹, P. Zhao², C. T. Kelley¹ and D. L. Woolard^{2,3}

¹Center for Research in Scientific Computation and Department of Mathematics

²Electrical and Computer Engineering Department

North Carolina State University, Raleigh, North Carolina, 27695-8205

³U.S. Army Research Office

U.S. Army Research Laboratory, RTP, North Carolina, 27709-2211

Abstract — This paper presents theoretical results on instability processes that occur in the positive-differential-resistance region of nanoscale tunneling structures and reports on efforts to develop advanced numerical techniques for use in future optimization studies. These results were obtained from numerical implementations of the Wigner-Poisson electron transport model. Here, the primary focus of the reported research is on developing simulation methods that are adaptive to parallel-computing platforms. Together, these investigations demonstrate the high computational demands associated with modeling fully time-dependent phenomenon in resonant tunneling structures (RTS) and offer new numerical solutions for the rapid and efficient analysis of these types of problems. Furthermore, the simulation tools under development will enable future investigations into new quantum phenomenon that strongly influence instability processes in RTSs.

I. INTRODUCTION

Resonant tunneling diodes possess extremely fast response times and have been utilized as the gain element in oscillator sources at frequencies approaching 1 terahertz (THz). Unfortunately, the traditional implementation of an RTD oscillator (i.e., where the RTD is used as an extrinsic gain element) leads to low output powers that are on the order of microwatts [1]. The limited output power of the *extrinsic* RTD oscillator is directly a result of the broadband gain. Specifically, when an RTD device is embedded in an electrical circuit or cavity, there will be a tendency to induce current oscillations across the entire frequency-band where the gain exists. Hence, high-frequency output power will either be lost to unwanted spurious low-frequency modes or significantly scaled back due to reductions in device area (and therefore output current) that must be used to lower RTD capacitance to achieve low-frequency stabilization. These basic facts have motivated a theoretical search for an *intrinsic* RTD oscillator design

that utilizes a microscopic instability mechanism directly [2]. In fact, our most recent efforts have been towards the specification of a resonant tunneling structure (RTS) that will yield current oscillations within the positive-differential-resistance region of the average current-voltage (I-V) characteristic. This particular scheme holds promise because it has the potential to realize a device with an intrinsic instability mechanism that will not produce oscillation modes outside a narrow prescribed domain. Hence, it may be possible to practically implement such an intrinsic RTS oscillator circuit without reducing the device contact area (along with the output current and power) as was needed for the low-frequency stabilization of the extrinsic RTD oscillator.

Very recent simulation studies performed upon emitter engineered RTSs suggest that it may be possible to induce current oscillations within the PDR region of the average I-V characteristic [3]. Specifically, a Wigner-Poisson model was utilized to study the electron dynamics of an RTS with an emitter engineered region as shown in Fig. 1. Here, the fractional compositions of the $\text{Ga}_{1-y}\text{Al}_y\text{As}$

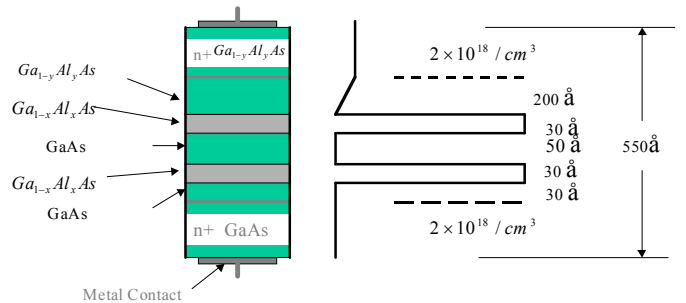


Fig. 1. Details of an emitter-engineered (EE) RTS.

material in the emitter region have been graded to prematurely induce an emitter quantum well (EQW) within the undoped portion of device in front of the first

barrier. This was done to alter the multi-subband structure that couples the EQW to the main quantum-well (MQW) of the RTD under a condition of applied bias. The goal of this particular engineering is to encourage a certain type of subband-coupling between the EQW and MQW which have been shown previously [3] to be the underlying instability mechanism for intrinsic oscillations in RTDs. The resulting average I-V curves for the RTS structure defined in Fig. 1 are given in Fig. 2. Note the emergence

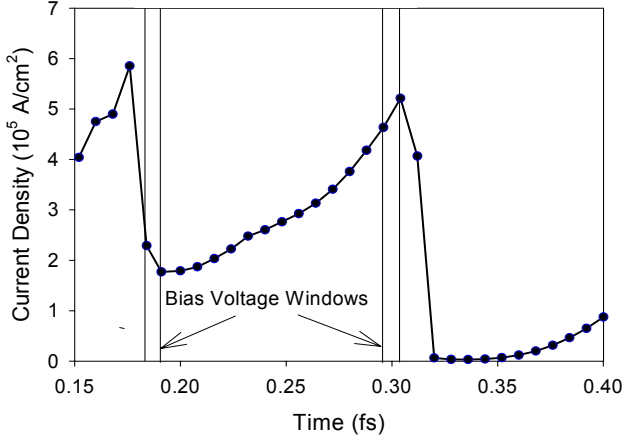
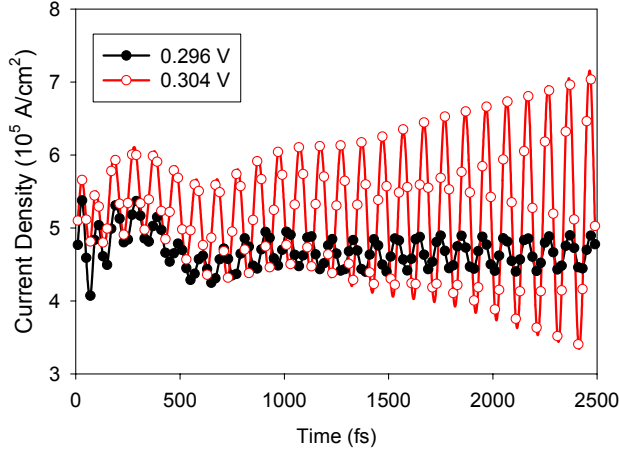


Fig. 2. Average I-V results for the EE-RTS in Fig. 1.

of two bias voltage windows (BVWs) with one residing in the PDR region. In addition, there is an enhancement in the amplitude of the current-density oscillation in the second BVW as shown in the results given in Fig. 3.



These

Fig. 3. Oscillation results for the second BVW in Fig. 2.

preliminary results suggest that it may be possible to design RTS-based oscillator circuits that do not induce extraneous low-frequency oscillations in the external

circuit. However, these simulations of the isolated RTS device are very computationally intensive and required over a week of runtime on a serial platform. Obviously, the full time-dependent simulation of the RTS device embedded in an oscillator circuit will require the use of efficient numerical tools on parallel computing platform. This paper will report on efforts to develop advanced numerical techniques for use in future optimization studies. Here, the emphasis is on the development of fast and efficient tools, that are adaptive to parallel computing platforms, and that can be used for future investigations into new quantum phenomenon that influence the operation of RTS-based oscillator circuits.

I. WIGNER-POISSON ELECTRON TRANSPORT MODEL

The Wigner function formulation of quantum mechanics was selected for these investigations into the RTS because of its many useful characteristics for the simulation of quantum-effect electronic devices, including the natural ability to handle dissipate and open-boundary systems. The Wigner function can be combined with the Poisson equation to provide for an adequate quantum mechanical description of the electron transport through tunneling nanostructures. Details regarding the derivation can be found elsewhere [4], but the model is a two equation system with the basic mathematical form

$$\frac{\partial f(x, k, t)}{\partial t} = W(f) \quad (1)$$

$$\frac{\partial^2 u(x)}{\partial x^2} = \frac{q^2}{\epsilon} [N_d(x) - n(x)] \quad (2)$$

where the last term in Eq. (1) is given by

$$W(f) = C_1 k \frac{\partial f}{\partial x} - K_0(f) + \frac{\partial f}{\partial t} \Big|_{coll} \quad (3)$$

with the physical constant $C_1 = -h/(2\pi m^*)$ and the integral expression defined by

$$K_0(f) = \frac{1}{h} \int_{-\infty}^{\infty} dk' f(x, k') T(x, k') \quad (4)$$

$$T(x, k') = \int_0^L dy [U(x+y) - U(x-y)] \sin(2y(k-k'))$$

where L is the length of the tunneling structure under consideration. The last term in Eq. (3) is due to scattering dissipation and is modeled using the relaxation time approximation [1]. The boundary conditions on $f(x, k')$ at the emitter ($x = 0$) and collector ($x = L$) are specified to approximate flat-band transport and equilibrium electron-distribution conditions [5].

III. TEMPORAL INTEGRATION ALGORITHMS

A. Integration Method - To track the time-evolution of the current density for a given value of applied bias voltage, the domain and equations are discretized and given to a numerical integrator, which accurately solves for the Wigner function, f , for given time interval over the discretized domain. So for a given time t , this method computes a vector f such that $(f)_{ij} \sim f(x_i, k_j, t)$, which is the discretized Wigner function over space and momentum coordinates. These approximations are computed over the coordinates, $x_i, i=1,2,\dots,N_x$ and $k_j, j=1,2,\dots,N_k$. Two separate methods were investigated and compared in terms of efficiency. While designing appropriate doping profiles, barrier well placement and widths, applied voltage biases, and other controllable physical parameters, several temporal simulations will be required. If the method is too inefficient, some design methods could be impractical to perform or even infeasible. The first integrator considered was ROCK4 [6]. ROCK4 is a fourth order Runge-Kutta method which incorporates variable stages to enhance the method's stability. ROCK4 is an explicit method, meaning the current solution calculated by the integrator is based only on previously computed data. Therefore, the advantage of this method is that it requires low storage and the solution can be quickly calculated from known values. The disadvantages of these methods are their stability regions. In order for the algorithm to remain stable, an explicit method is forced to take small time steps, forcing the integrator to do more work. The second method explored by the authors was VODEPK [7,8]. This method is a variable-order implicit method. Since it is implicit, at each time step a nonlinear equation must be solved to compute the current solution. While this is a disadvantage when compared to explicit methods, the implicit methods are allowed to take larger time steps since these methods are not concerned with satisfying stability constraints. So if the nonlinear equations could be solved effectively, then the implicit method could have an overall advantage over the explicit method.

B. Preconditioner Development - To solve the nonlinear equations that arise in the time integration, VODEPK uses a Newton-GMRES algorithm. This is an iterative method that finds the root of a nonlinear function $G : R^m \rightarrow R^m$ where the next iterate is found by stepping forward from the current iterate f_n . Note, for our problem, $m=N_x*N_k$ and f_n is the initial guess for the Wigner function at the current time. The step direction, s_n , solves the linear equation $G'(f_n)s_n = -G(f_n)$, where $G'(f_n)$ is the Jacobian matrix of G evaluated at f_n . Therefore, a linear equation must be solved for every Newton iterate. Here, the equation is solved with an iterative method called GMRES. This method does not require the computation of the coefficient matrix (i.e., Jacobian matrix in our case) or its storage, which is advantageous since as we refine the grids to get a more accurate simulation of the RTD, the dimension of this problem is expected to become quite large. Also, it has been well established that if a good preconditioner can be found, GMRES can efficiently find solutions to large systems of linear equations [9]. A preconditioner is another matrix, M , multiplied into the linear equation in hopes of better conditioning the Jacobian matrix, hence accelerating the convergence of GMRES. So GMRES would solve the linear equation $MG'(f_n)s_n = -G(f_n)$, where $MG'(f_n)$ would be a better-conditioned coefficient matrix than the usual $G'(f_n)$. The Newton iteration successfully terminates when either the size of the next step is below a set tolerance, or norm of the nonlinear function is below a set tolerance. Note that both of these parameters will be approaching a very small value if the algorithm is converging to the correct answer. When applying VODEPK to the Wigner equation, the Jacobian matrix of the nonlinear equations in VODEPK have the form $G'(f) = I - A \cdot \partial W(f) / \partial f$, where A is some constant. If we ignore all the terms in $W(f)$ except the $D_x(f)$ term, then we get that $\partial W(f) / \partial f \approx D_x$. Therefore, a good preconditioning matrix would be $M = (I - AD_x)^{-1}$ since $G'(f)^{-1} \approx (I - AD_x)^{-1}$. This preconditioner is also computationally inexpensive to implement since the matrix representation of D_x is sparse.

C. Numerical Results and Statistics - The new integration algorithms were implemented and tested in our base simulation code [10] used to derive the results given in Section I. It is important to note that the original code utilizes a coherence length, L_c , that is tied to the upper value of the x -space grid. Hence, it is also important to monitor the value of L_c as we refine the grid. The table below summarizes the serial runtimes of the ROCK4 and VODEPK version of the simulations on several different grids. Note that all of the computations were performed on the IBM-SP3 at the North Carolina Supercomputing

Center (NCSC). The runtimes below suggest that VODEPK handles time integration more efficiently than ROCK4, especially as the grids are refined. So VODEPK has been chosen for our future simulation since its performance will be better for generating accurate solutions to larger dimensional problems. Figure 4 shows the average I-V curves for the (N_x, N_k) grids of (86,72) and (64,128). Note, the (86,72) grid results exactly duplicate

Table I. CPU Time versus

N_x	N_k	ROCK4 (min)	VODEPK (min)	L_c (Å)	Δx (Å)	Δk (m/Å)
32	32	10	5	550	17.8	5.5
32	64	40	60	1118	17.8	2.8
64	64	124	108	550	8.7	5.6
86	72	294	58	459.4	6.5	6.7
64	128	432	365	1109	8.7	2.8

simulations that were made with the original code – see previously published results in [10]. The (86,72) grid results in Fig. 4 are in almost exact agreement with those generated earlier with the original code; however, the new simulator obtained the results approximately 100 times faster. Note also that the results in Fig. 5 show that the overall results are strongly influenced by the value of L_c . Hence, future work will focus on investigating the effects that both the coherence length and the applied bias voltage has on creating and sustaining current oscillations in engineered RTs. Furthermore, the physically appropriate value of L_c will be determined through comparisons to experimental results.

IV. CONCLUSION

The results of these computational studies have demonstrated an advanced numerical algorithm for the fast and efficient study of resonant tunneling structures.

REFERENCES

- [1] D. L. Woolard et. al., “Advanced Theoretical Techniques for the Study of Instability Processes in Nanostructures,” Chapter 8 in *Terahertz Sensing Technology, Volume II*. (World, Scientific, 2003).
- [2] D. Woolard, P. Zhao and H.L. Cui, “THz-Frequency Intrinsic Oscillations in Double-Barrier Quantum Well System,” *Physica B* **314** pp. 108-112, 2002.
- [3] P. Zhao, D. L. Woolard and H. L. Cui, “Multisubband Theory for the Origination of Intrinsic Oscillations within Double-barrier Quantum Well Systems,” *Phys. Rev. B* **67**, 085312, 2003.

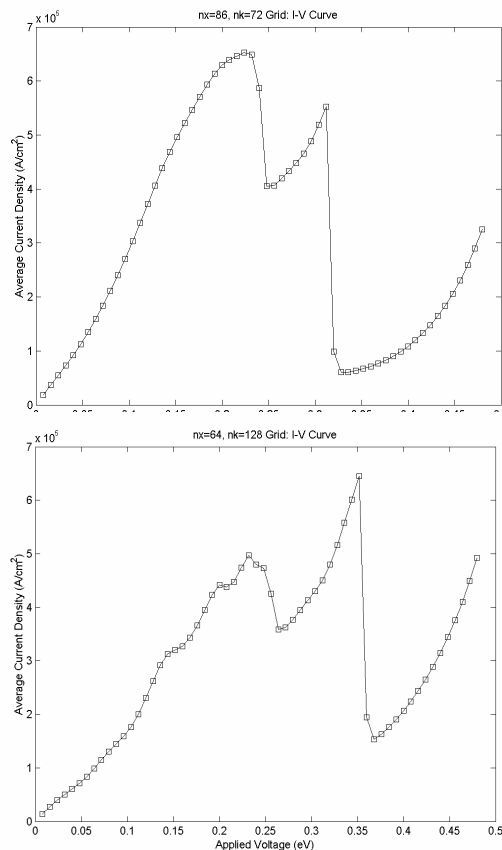


Fig. 5. Average I-V results for: (a) (86,72), and (b) (64,128), grids.

- [4] C. T. Kelley, et. al., “Parallel-Platform Based Numerical Simulation of Instabilities in Nanoscale Tunneling Devices,” in *IEEE NANO Conf. Proceedings* (2002).
- [5] K. L. Jensen and F. A. Buot, *Phys. Rev. Lett.* **66**, 1078 1991.
- [6] Assyr Abdulle, “Fourth Order Chebyshev Methods with Recurrence Relation,” *SIAM Journal on Scientific Computing*, **23**(6) pp. 2041-2054 (2002).
- [7] P. N. Brown, G. D. Byrne and A. C. Hindmarsh, “VODE, A Variable-Coefficient ODE Solver,” Tech. Report, UCRL-98412, Lawrence Livermore Lab. (1988).
- [8] P. N. Brown and A. C. Hindmarsh, “Reduced Storage Matrix Methods in Stiff ODE Problems,” Tech. Report, UCRL-95088, Lawrence Livermore Lab. (1987).
- [9] C. T. Kelley, “Iterative Methods for Linear and Nonlinear Equations,” Vol. 16 of *Frontiers in Applied Mathematics* (SIAM, Philadelphia, 1995).
- [10] P. Zhao, H. L. Cui and D. L. Woolard, “Dynamical Instabilities and I-V Characteristics in Resonant Tunneling Through Double Barrier Quantum Well Systems,” *Phys. Rev. B* **63** 75302 (2001).